https://journals.unizik.edu.ng/ujcee

Unizik Journal of Chemical & Environmental Engineering

Volume 1, Issue 1, Pages 052-068
2026

Received: 02.06.2026
Accepted: 04.07.2026
Published: 10.07.2026

Sustainable Removal of Phenol from PharmaceuticalWastewater Using Carbonized Rice Husk: Modeling and Optimization via RSM

Lawrence Ifeanyi Igbonekwu [1], **Matthew Ndubuisi Abonyi** [2*]

[1] Department of chemical engineering, Nnamdi Azikiwe University, Awka; Li.igbonekwu@unizik.edu.ng
[2] Department of chemical engineering, Nnamdi Azikiwe University, Awka; mn..abonyi@unizik.edu.ng
* Correspondence: mn..abonyi@unizik.edu.ng

Abstract

This study investigates the sustainable removal of phenol from real pharmaceutical wastewater using carbonized rice husk (RH) as a low-cost agro-waste-derived adsorbent. The adsorbent was prepared through combined thermal and chemical activation to enhance surface properties, and its characteristics were examined using scanning electron microscopy (SEM) and Fourier transform infrared spectroscopy (FTIR). Batch adsorption experiments were conducted to evaluate the effects of pH, adsorbent dosage, contact time, temperature, and initial phenol concentration. Equilibrium data were best described by the Langmuir isotherm model (R^2 = 0.9872), indicating monolayer adsorption with a maximum adsorption capacity of 66.5 mg/g. Kinetic analysis showed that the pseudo-secondorder model (R^2 = 0.9805) provided the best fit, suggesting that adsorption is governed by surface interactions. Thermodynamic parameters revealed that the adsorption process is spontaneous and exothermic, with ΔG values ranging from –12.73 to –10.76 kJ/mol and ΔH = –37.98 kJ/mol. Response Surface Methodology (RSM) based on Central Composite Design (CCD) was employed to model and optimize the adsorption process. The model was statistically significant ($F = 21.40$, $p < 0.0001$) with a high coefficient of determination (R^2 = 0.9365). Optimal conditions resulted in a maximum phenol removal efficiency of 99.83%. The findings demonstrate that carbonized rice husk is an efficient, sustainable, and economically viable adsorbent for phenol removal from complex wastewater systems, with strong potential for practical application and scale-up.

Keywords: Phenol removal; Carbonized rice husk; Pharmaceutical wastewater; Adsorption, Response surface methodology; Isotherm, kinetics; Wastewater treatment.

Introduction

The rapid growth of industrial and pharmaceutical activities has led to the continuous discharge of hazardous organic pollutants into aquatic environments, posing serious threats to both ecological systems and human health (Khan et al., 2022). Among these pollutants, phenol and its derivatives are of particular concern due to their high toxicity, persistence, and potential carcinogenic effects, even at low concentrations (Hammam, Zaki, Yousef, & Fawzi, 2015). Phenolic compounds are

commonly found in effluents from pharmaceutical, petrochemical, resin, and plastic industries, and their uncontrolled release into water bodies can lead to severe environmental issues, including disruption of aquatic life and contamination of potable water sources.

Conventional treatment methods for phenol removal, such as chemical oxidation, coagulation–flocculation, membrane filtration, ion exchange, and advanced oxidation processes, have been widely investigated (Villegas et al., 2016). However, these techniques are often limited by high operational costs, sludge generation, energy requirements, and reduced efficiency at low pollutant concentrations (da Silva Aires et al., 2024). In contrast, adsorption has emerged as one of the most effective and economically viable techniques for phenol removal due to its simplicity, high efficiency, and adaptability to a wide range of operating conditions.

Activated carbon remains the most widely used adsorbent for phenol removal; however, its high production and regeneration costs limit its large-scale application, particularly in developing countries (Dąbrowski, Podkościelny, Hubicki, & Barczak, 2005). Consequently, there has been increasing interest in the development of low-cost, sustainable adsorbents derived from agricultural wastes. Rice husk (RH), an abundant agro-industrial by-product in rice-producing regions, has attracted considerable attention due to its high carbon and silica content, availability, and low economic value. Despite its potential, the effective utilization of rice husk as an adsorbent requires appropriate modification techniques to enhance its surface properties and adsorption capacity (Mishra, Dhada, Haldar, & aspects, 2023).

Several studies have explored the use of rice husk and other agricultural wastes for phenol adsorption. However, most of these studies are limited to either synthetic wastewater systems or single-factor experimental approaches, which fail to adequately capture the complex interactions between process variables in real wastewater environments. In addition, limited attention has been given to the combined effects of multiple operating parameters using robust statistical optimization tools, particularly when treating actual pharmaceutical effluents.

To address these limitations, Response Surface Methodology (RSM) has been increasingly employed as an efficient statistical tool for modeling and optimization of multivariable systems (Reji & Kumar, 2022). RSM enables the evaluation of individual and interactive effects of process parameters while minimizing experimental runs (Reji & Kumar, 2022). Nevertheless, there remains a significant gap in the application of RSM for optimizing phenol removal using modified rice husk in real pharmaceutical wastewater systems, especially when multiple critical variables are simultaneously considered.

Therefore, this study aims to investigate the adsorption performance of carbonized rice husk for the removal of phenol from pharmaceutical wastewater, while employing a Central Composite Design (CCD) within the framework of RSM to model and optimize the process. The novelty of this work lies in the integration of (i) dual activation (thermal and chemical) of rice husk to enhance adsorption efficiency, (ii) application of a five-factor CCD to capture complex interactions among operational variables, and (iii) utilization of real pharmaceutical wastewater rather than synthetic solutions, thereby improving the practical relevance of the findings. This approach provides a more comprehensive understanding of the adsorption system and offers a scalable, cost-effective solution for sustainable wastewater treatment.

Materials and Methods

2.1 Wastewater Sample Collection and Preservation

Pharmaceutical wastewater samples were collected from the effluent discharge unit of a pharmaceutical industry located in Awka, Anambra State, Nigeria. The samples were obtained in clean, airtight polyethylene containers and transported immediately to the laboratory for analysis. The initial pH of the wastewater was measured in situ using a calibrated digital pH meter. To prevent biodegradation prior to experimentation, the samples were preserved at 4 °C

in a refrigerator, following standard procedures for wastewater handling.

2.2 Preparation of Adsorbent

2.2.1 Pre-treatment of Rice Husk

Raw rice husk (RH) was collected from Achalla, Anambra State, Nigeria. The material was thoroughly washed with distilled water to remove adhering dust and impurities, followed by oven drying at 105 °C for 24 h to eliminate moisture. The dried sample was sieved to obtain a uniform particle size of 150 µm and stored in airtight containers for further use.

2.2.2 Thermal Activation

The pre-treated rice husk was subjected to carbonization in a muffle furnace at 400 °C for 2 h under limited oxygen conditions to produce char. This process enhanced pore development and increased the surface area of the adsorbent.

2.2.3 Chemical Activation

The carbonized rice husk was chemically activated using orthophosphoric acid (H_3PO_4). A 1:1 impregnation ratio (w/v) was used with 3 M H_3PO_4, and the mixture was allowed to stand for 24 h to ensure proper penetration of the activating agent. The sample was subsequently washed with distilled water until a neutral pH (~7) was attained, then oven-dried at 105 °C for 6 h. The prepared adsorbent was stored in desiccators for further experiments.

2.3 Batch Adsorption Experiments

Adsorption experiments were conducted in batch mode to evaluate the removal efficiency of phenol under varying operational conditions using 250 mL of pharmaceutical wastewater in 500 mL conical flasks. The effects of adsorbent dosage (0.25-3.25 g), pH (3-12), temperature (23-73 °C), initial phenol concentration (5-65 mg/L), and contact time (5-65 min) were investigated based on a Central Composite Design (CCD). A measured mass of carbonized rice husk was added to the wastewater of known initial phenol concentration. The solution pH was adjusted using 0.1 M NaOH or 0.1 M HCl. The mixture was agitated at 300 rpm and maintained at the desired temperature using a thermostatic hot plate. At predetermined time intervals, samples were withdrawn, filtered using Whatman No. 1 filter paper, and analyzed for residual phenol concentration using a UV-Vis spectrophotometer at 270 nm. All experiments were conducted in triplicate, and the adsorption capacity (qe), (qt) and percentage removal efficiency (%RE) were calculated using Eqs. (1)-(3).

$$q_e = \frac{\left(C_{o-C_e}\right)v}{w} \quad (1)$$

$$q_e = \frac{\left(C_{o-C_t}\right)v}{w} \quad (2)$$

$$\Re(\%) = \frac{\left(C_{o-C_e}\right)v}{w} \times 100 \quad (3)$$

where q_e is the equilibrium adsorption capacity per gram of dry weight of the adsorbent, (mg/g): qt is the adsorption capacity at time, t (mg/g): C_0 is the initial concentration of phenol in the solution (mg/L); C_e is the final or equilibrium concentration of phenol in the solution (mg/L); C_t is the amount of phenol adsorbed at time, t (mg/L); V is the volume of the solution (L); and W is the dry weight of adsorbent (g).

2.4 Equilibrium Studies

There are several isotherm equations available for analyzing experimental sorption equilibrium parameters, the most common being the Langmuir and Freundlich models.

2.4.1 The Langmuir isotherm

The Langmuir isotherm model is predicated on the idea that the adsorbent's surface contains a uniform distribution of a finite number of active sites. There is no interaction between the adsorbed molecules and these active sites have the same affinity for the adsorption of a micromolecular layer (Langmuir, 1918). In addition to being used to compare and measure the adsorptive capacities of different adsorbents, its main purpose was to explain gas-solid phase adsorption (Elmorsi, 2011). By maintaining a balance between the relative rates of adsorption and desorption (dynamic equilibrium), the Langmuir isotherm explains the surface coverage. There are two

ways to express the Langmuir equation: linear and nonlinear.

$$q_e = \frac{qmKLCe}{1+KLCe} \quad (4)$$

$$\frac{C_e}{q_e} = \frac{1}{q_m k_L} + \frac{C_e}{q_m} \quad (5)$$

Where C_e is the concentration of adsorbate at equilibrium (mg/g), K_L is Langmuir constant related to adsorption capacity (L/mg), which can be correlated with the variation of the suitable area and porosity of the adsorbent which implies that large surface area and pore volume will result in higher adsorption capacity, q_m is the maximum adsorption capacity for a complete monolayer coverage.

2.4.2 The Freundlich Isotherm

The Freundlich is applicable to adsorption processes that occur on heterogenous surfaces (Ayawei, Ebelegi, & Wankasi, 2017). It also gives an expression which defines the surface heterogeneity and the exponential distribution of active sites and their energies (Ayawei et al., 2017). The linear and non lineear form of the Freundlich isotherm are as follows;

$$q_e = k_f C_e^{(1/n)} \quad (6)$$

$$\log q_e = \log k_f + \frac{1}{n} \log c_e \quad (7)$$

Where K_F is adsorption capacity (L/mg) and $1/n$ is adsorption intensity; it also indicates the relative distribution of the energy and the heterogeneity of the adsorbate sites. The values of n in the range of 2-10 represent good adsorption, 1-2 moderate adsorptions and less than 1 represents poor adsorption characteristics (Húmpola, Odetti, Fertitta, & Vicente, 2013).

2.4.3 Temkin Isotherm

One of the earliest isotherms to be described, the Temkin isotherm suggests that the interactions between the adsorbent and adsorbate causes the heat of adsorption to decrease linearly with increasing coverage. According to Temkin (Temkin, 1940), the nonlinear and linearized forms of the Temkin isotherm have typically been utilized in the forms shown in Eqs. 8 and 9, respectively.

$$q_e = \frac{RT}{BT} \ln \left(K_T C_e \right) \quad (8)$$

$$q_e = \frac{RT}{BT} \ln K_T + \frac{RT}{BT} \ln C_e \quad (9)$$

Where: K_T (lg^{-1}) is the Temkin isotherm constant, b_T ($Jmol^{-1}$) is a constant related to the heat of sorption and R ($8.314 Jmol^{-1}K^{-1}$) is the gas constant.

2.5 Kinetic studies

Adsorption mechanisms are evaluated by applying the major adsorption kinetic models. In this research work, three kinetic models (pseudo-first order, pseudo-second order, and Elovich model) were applied to the experimental data to investigate the kinetics of sorption of phenol on RH. First and second order assumed the adsorption process to be pseudo-chemical in nature, while Elovich model is applied to explain whether adsorption is physical adsorption or chemisorption (Rengaraj, Moon, Sivabalan, Arabindoo, & Murugesan, 2002). The linear form of Lagergren's first-order rate equation is as follows (Yuh-Shan, 2004).

$$\log (q_e - q_t) = \log q_e - \frac{K_{p1}}{2.303} t \quad (10)$$

where qe is the amount of phenol adsorbed onto the adsorbent at equilibrium (mg/g), qt is the amount of phenol adsorbed onto the adsorbent at any time t (mg/g), and Kp_1 (min^{-1}) is the rate constant of the pseudo-first-order adsorption which can be calculated from the slope of the linear plot of ln(qe − qt) vs. t The linearized form of the pseudo-second-order model is given as

$$\frac{t}{q_t} = \frac{1}{k_2 q_e^2} + \frac{1}{q_t} t \quad (11)$$

Where the slope and intercept of the plot of t/qt versus t can be used to experimentally calculate the equilibrium adsorption capacity (qe) and the second order constants k_2 (g/mg h).

Results and Discussion

The physicochemical properties of the prepared rice husk (RH) adsorbent are presented in Table 1. The low moisture content (2.3%) indicates good thermal stability and suitability for adsorption applications (Chulliyil et al., 2024). The developed porous structure and appreciable surface area suggest the availability of active sites for phenol uptake.

Table 1: Characterization result of RH

Adsorbents	Moisture content (%)	Surface area (cm^2)
RH	2.3	94.8

3.1 Scanning Electron Microscopy Result

The SEM micrographs of the rice husk (RH) adsorbent before and after phenol adsorption show notable changes in surface morphology, confirming the occurrence of adsorption. Prior to adsorption, the RH surface exhibits a rough and heterogeneous texture characterized by irregular pores, cracks, and cavities, indicating a well-developed porous structure suitable for adsorption. These features provide a large surface area and numerous active sites for phenol uptake. After adsorption, the SEM image shows a comparatively smoother and more compact surface, with visible reduction in pore volume and partial blockage of cavities. The morphological transformation observed between the fresh and spent RH confirms the effective interaction between phenol molecules and the adsorbent surface, indicating successful adsorption.

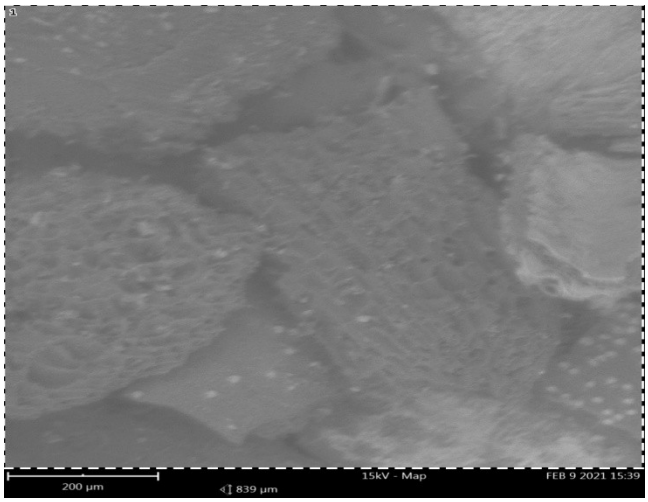

Plate 1. SEM of RH before adsorption

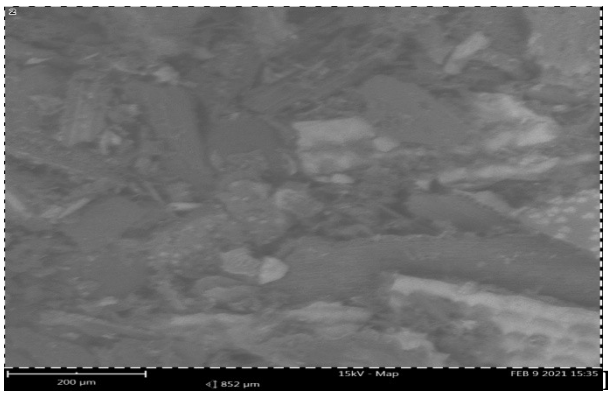

Plate 2. SEM of RH after adsorption

3.2 Fourier Transform Infrared Result

The FTIR spectra of the rice husk (RH) adsorbent before and after phenol adsorption reveal distinct changes in peak positions and intensities, indicating the involvement of surface functional groups in the adsorption process. In the spectrum of the raw RH, a broad absorption band observed in the region of approximately 3200–3600 cm^{-1} is attributed to the stretching vibrations of hydroxyl (–OH) groups, which are characteristic of alcohols and phenolic structures (Coates, 2000). Peaks around 2900 cm^{-1} correspond to aliphatic C–H stretching vibrations (Stuart, 2004). The presence of a band near 1700 cm^{-1} suggests C=O stretching of carbonyl or carboxylic groups, while peaks within the range of 1000–1200 cm^{-1} are assigned to C–O and Si–O stretching vibrations, indicating the lignocellulosic and silica-rich nature of the adsorbent (Coates, 2000; Stuart, 2004). After phenol adsorption, noticeable shifts in the –OH stretching region and changes in peak intensities were observed, suggesting the involvement of hydroxyl groups in hydrogen bonding interactions with phenol molecules (Hameed & Rahman, 2008). Additionally, slight shifts in the C–O and Si–O bands indicate possible interaction between phenol and oxygen-containing functional groups on the adsorbent surface (Foo & Hameed, 2010). The observed spectral changes confirm that functional groups such as –OH, C=O, and Si–O play significant

roles in the adsorption process, indicating that phenol uptake occurs through a combination of hydrogen bonding and surface interactions.

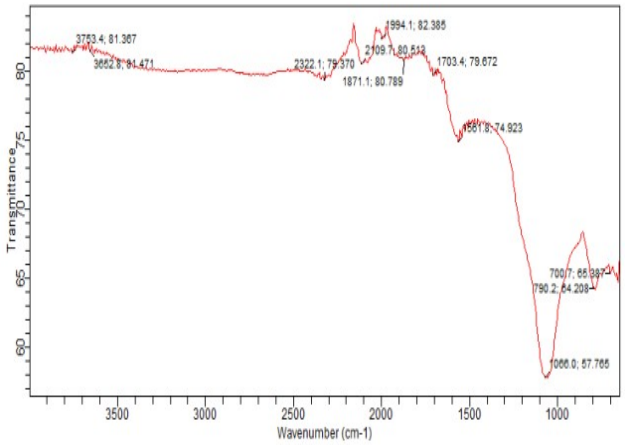

Figure 1: FTIR spectra of RH before adsorption

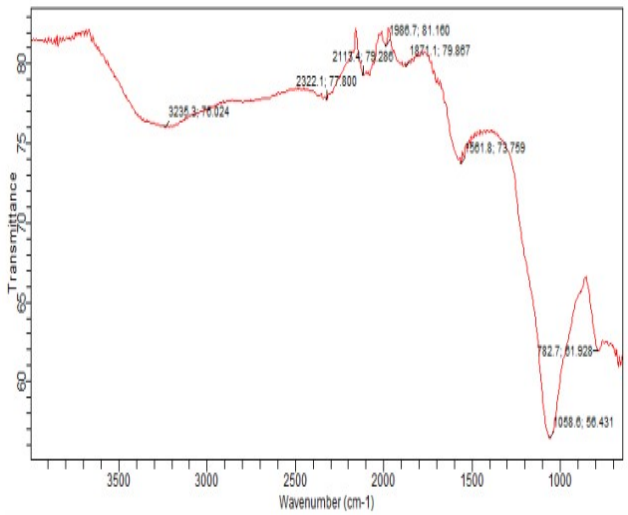

Figure 2: FTIR spectra of RH after adsorption

3.3 Influence of Adsorbent Dosage and Contact Time

Figure 3 presents the effect of adsorbent dosage (1.0-2.5 g) and contact time (10-55 min) on the percentage removal of phenol using rice husk (RH). As shown, phenol removal increased progressively with increasing adsorbent dosage at all contact times investigated. Specifically, the removal efficiency improved from approximately 78.85% at 1.0 g to a maximum of 84.99% at 2.5 g. The increase in adsorption efficiency with dosage is attributed to the corresponding increase in available active sites and surface area for phenol uptake (Lin, Pan, Chen, Cheng, & Xu, 2009). However, the improvement in removal efficiency becomes marginal beyond 2.0 g, where the increase from 2.0 g to 2.5 g resulted in only a slight enhancement in adsorption. This behavior may be due to partial aggregation of adsorbent particles at higher dosages, leading to reduced effective surface area and overlapping of active sites (Wang, Shi, Pan, Zhang, & Zou, 2020). Similarly, contact time significantly influenced the adsorption process. A rapid increase in phenol removal was observed within the initial stages of adsorption (10-35 min), indicating fast occupation of readily available surface sites. Beyond 35 minutes, the adsorption rate gradually approached equilibrium, with minimal changes in removal efficiency up to 55 minutes. This trend suggests that adsorption is initially surface-controlled and subsequently limited by the availability of remaining active sites.

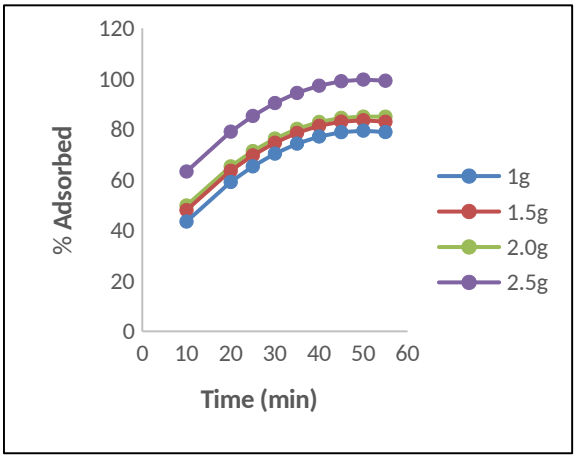

Figure 3: Influence of Adsorbent (RH) Dosage and Contact Time

3.4 Influence of Effluent Temperature on Phenol Adsorptive Rate

Figure 4 illustrates the effect of effluent temperature (298-333 K) and contact time (10-55 min) on the adsorption of phenol onto RH. As observed, phenol removal efficiency decreased with increasing temperature across all contact times. The highest adsorption performance was recorded at 308 K, with removal efficiency reaching approximately 92.05%, while a noticeable decline

was observed at higher temperatures, dropping to about 65.99% at 333 K. The decrease in adsorption efficiency with increasing temperature indicates that the adsorption process is exothermic in nature (Chen, Zhao, Wu, & Dai, 2011). At lower temperatures, the interaction between phenol molecules and the adsorbent surface is stronger, promoting adsorption. However, as temperature increases, the kinetic energy of phenol molecules also increases, weakening the adsorptive forces and enhancing the tendency of adsorbed molecules to desorb back into the solution (Chen et al., 2011). In addition, the adsorption profiles at different temperatures show a rapid increase in phenol uptake within the initial contact period (10-35 min), followed by a gradual approach to equilibrium. This trend suggests that adsorption is initially governed by surface interactions and becomes progressively limited by the availability of active sites.

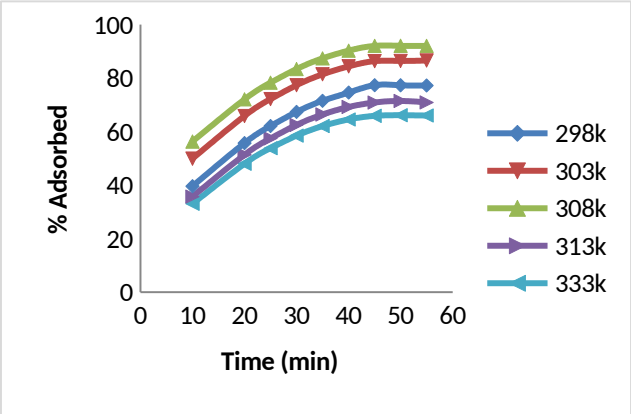

Figure 4: Effect of temperature and contact time on phenol adsorption onto RH

3.5 Influence of Pharmaceutical effluent pH on Phenol Adsorptive Rate

Figure 5 presents the effect of solution pH (3-12) and contact time (10-55 min) on phenol adsorption onto RH. The results show that phenol removal increased from approximately 81.02% at pH 3 to a maximum of about 91.46% at pH 5, after which a gradual decline was observed, decreasing to approximately 74.16% at pH 6 and further to 69.63% at pH 10. The initial increase in adsorption efficiency from pH 3 to 5 can be attributed to reduced competition between hydrogen ions and phenol molecules for active sites on the adsorbent surface (Beker, Ganbold, Dertli, Gülbayir, & Management, 2010). At moderately acidic conditions (pH 5), the surface of the adsorbent favors interaction with phenol molecules, resulting in enhanced adsorption. However, beyond pH 5, the decrease in removal efficiency is likely due to increased ionization of phenol and the higher concentration of hydroxide ions (OH^-) in solution (Beker et al., 2010). These factors lead to electrostatic repulsion between the negatively charged adsorbent surface and phenolate ions, thereby reducing adsorption efficiency. In addition, adsorption profiles at all pH values show a rapid increase in phenol uptake within the initial contact period (10-35 min), followed by a plateau up to 55 min, indicating that equilibrium was attained. This suggests that adsorption is initially controlled by surface interactions and later limited by the availability of active sites.

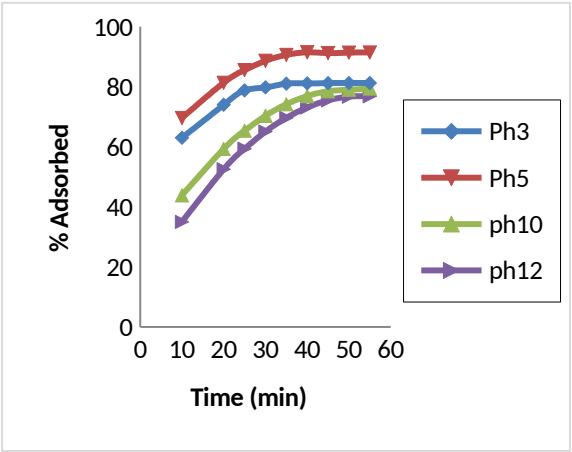

Figure 5: Effect of solution pH and contact time on phenol adsorption onto RH

3.6 Effect of Initial Phenol Concentration

Figure 6 illustrates the effect of initial phenol concentration (25-45 mg/L) and contact time (10-55 min) on the adsorption of phenol onto RH. The results indicate that phenol removal efficiency decreased with increasing initial concentration at all contact times. Specifically, the removal efficiency declined from approximately 83.92% at 25 mg/L to 74.17% at 35 mg/L, and further to about 66.27% at 45 mg/L. The observed decrease in percentage removal with increasing initial concentration can be attributed to the saturation of

available adsorption sites on the adsorbent surface. At lower concentrations (25 mg/L), the ratio of available active sites to phenol molecules is high, resulting in more efficient adsorption. However, as the concentration increases, the number of phenol molecules exceeds the available binding sites, leading to reduced removal efficiency. In addition, the adsorption profiles show a rapid increase in phenol uptake within the initial contact period (10-35 min), followed by a gradual plateau up to 55 min, indicating that equilibrium was attained. This behavior suggests that adsorption is initially controlled by surface interactions and subsequently limited by site saturation.

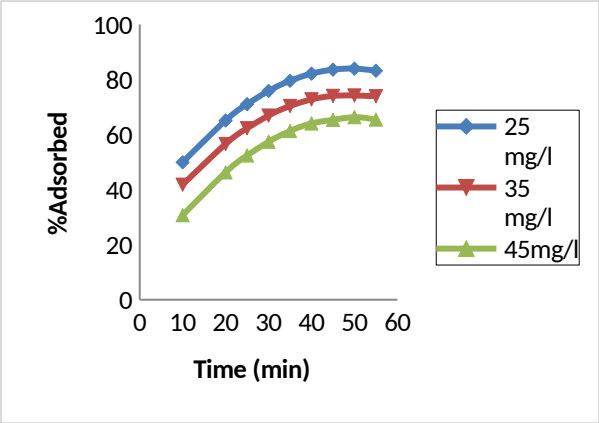

Figure 6: Effect of initial phenol concentration and contact time on adsorption onto RH

3.7 Adsorption Isotherm Studies

The equilibrium adsorption data for phenol removal onto RH were analyzed using Langmuir, Freundlich, and Temkin isotherm models, and the corresponding parameters are presented in Table 2. The Langmuir isotherm model exhibited the best fit to the experimental data with a high correlation coefficient (R^2 = 0.9872), indicating monolayer adsorption of phenol onto a homogeneous adsorbent surface. The maximum adsorption capacity (q_m) was determined to be 66.5 mg/g, suggesting that RH possesses a high affinity for phenol uptake (Langmuir, 1918). The Langmuir constant (K_L = 1.29 L/mg) which reflect the affinity between the adsorbent and adsorbate, indicating strong interaction between phenol molecules and the adsorbent surface (Langmuir, 1918). The dimensionless separation factor (R_L = 0.96) lies within the range ($0 < R_L < 1$), indicating that the adsorption process is favorable. This confirms the suitability of the Langmuir model in describing the adsorption behavior. (Hall, Eagleton, Acrivos, Vermeulen, & fundamentals, 1966)

Table 2: Linear equilibrium isotherm parameters for phenols adsorption onto adsorbent

Adsorption	Isotherm	H	R
Langmuir	q_m(mg/g)	6.5	6
	K_L(L/mg)	29	1.
	R_L		0.
		96	
	R_2		0.98
Freundlich	n_F	72	0.
		69	
	K_f(L/mg)		239
		.56	
	R^2		0.9
		811	

The Freundlich isotherm model also showed good agreement with the experimental data, with a correlation coefficient of R^2 = 0.9811, indicating heterogeneous surface adsorption (Ayawei et al., 2017). The Freundlich constant (K_F = 239.56 L/mg) reflects a relatively high adsorption capacity, while the value of (n = 0.69) suggests that the adsorption process involves non-ideal adsorption behavior, indicating strong interaction between phenol molecules and the adsorbent surface (Ayawei et al., 2017).

In contrast, the Temkin isotherm model showed a lower correlation coefficient (R^2 = 0.9165), indicating a comparatively weaker fit. This suggests that the assumption of linear decrease in adsorption heat with surface coverage is less applicable to the present system (Temkin, 1940).

In all, the superior performance of the Langmuir model compared to Freundlich and Temkin models confirms that phenol adsorption onto RH predominantly occurs as monolayer coverage on a relatively homogeneous surface, with strong adsorbate-adsorbent interactions.

Temkin	B_T	43.682
	A_T(l/g)	8.620
	R^2	0.9165

3.8 Kinetic Studies

The adsorption kinetics of phenol onto RH were evaluated using pseudo-first-order, pseudo-second-order, and Elovich models, and the corresponding parameters are presented in Table 3. The pseudo-second-order model provided the best fit to the experimental data with the highest correlation coefficient (R^2 = 0.9805) compared to the pseudo-first-order (R^2 = 0.9231) and Elovich (R^2 = 0.9421) models. This indicates that the adsorption process is predominantly governed by surface interactions involving the adsorbent and adsorbate (Y.-S. Ho & McKay, 1999).

The rate constant for the pseudo-second-order model (k_2 = 0.0569 L/mg·min) further supports the suitability of this model in describing the adsorption kinetics. The relatively high agreement between the model and experimental data suggests that the rate-limiting step may involve adsorption at active sites on the adsorbent surface (Y.-S. J. J. o. h. m. Ho, 2006).

Although the pseudo-first-order model showed moderate agreement, its lower correlation coefficient indicates that it is less suitable for describing the adsorption behavior of phenol onto RH (Lagergren, 1898). Similarly, the Elovich model, which is often associated with adsorption on heterogeneous surfaces, also showed a lower correlation, suggesting that it does not adequately represent the adsorption kinetics in this study (Rengaraj et al., 2002).

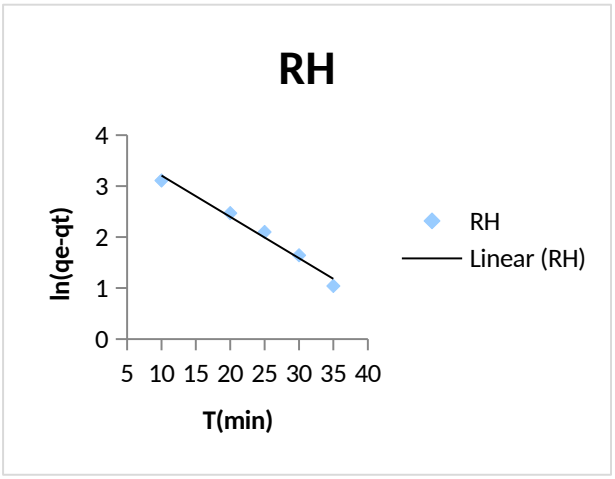

Figure 7: Linear pseudo first order kinetic plot

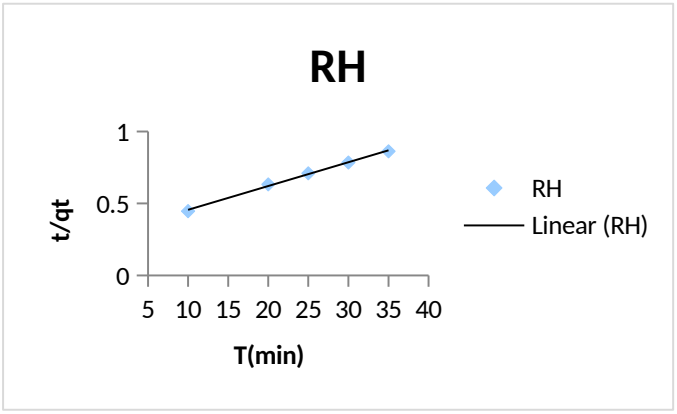

Figure 8: Linear pseudo second order kinetic plot

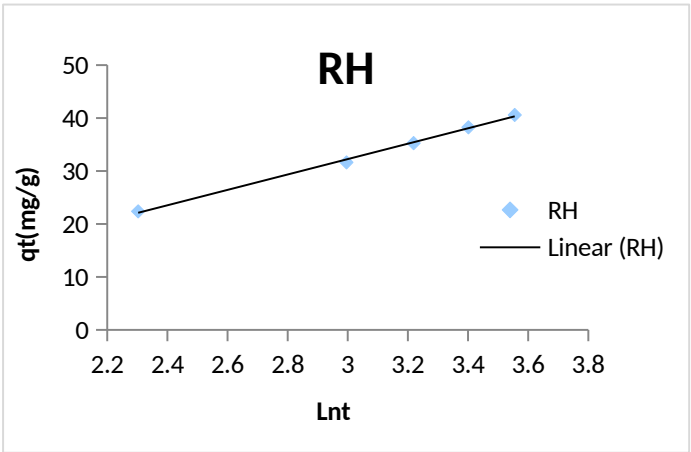

Figure 9: Linear Elovich Kinetic Plot

Table 3: Linear kinetic parameters for phenol adsorption onto adsorbents

Adsorption kinetics	RH
Pseudo-first	

order	K_1 (min^{-1})	0.081
	R^2	0.9231
Pseudo second order	K_2 (L/mg.min)	0.0569
	R^2	0.9805
Elovich	α (mg/g.min)	0.4584
	β (g/mg)	0.0688
	R^2	0.9421

3.9 Response Surface Result

The adsorption of phenol using rice husk (RH) was investigated through a Central Composite Design (CCD) involving five key process parameters: dosage (A), pH (B), temperature (C), initial phenol concentration (D), and contact time (E). The design matrix as presented in table 4, comprised 50 experimental runs, with actual and predicted removal efficiencies ranging from as low as 25.85% to as high as 99.83%. A close agreement between experimental and predicted values across most runs indicates that the model accurately describes the system behavior, with only minor deviations observed in a few runs (e.g., run 10 and run 30), suggesting good model fit and minimal experimental noise.

Table 4.CCD Design Matrix for RH

Run	A:dosage (g)	B:pH	C: Temp (°C)	D:conc. (mg/L)	E:Time (min)	Actual (%)	Predicted (%)
1	1.75	8	48	35	35	82.30	81.32
2	0.25	8	48	35	35	61.02	62.28
3	1.75	8	48	35	5	51.2	48.63
4	1	4	60	20	50	48.44	49.16
5	2.5	4	60	50	20	60.11	60.02
6	1.75	8	48	65	35	99.18	101.26
7	1.75	12	48	35	35	74.44	83.45
8	1.75	8	48	5	35	67.70	66.80
9	1.75	8	48	35	35	82.3077	81.32
10	1	12	35	20	20	41.4359	52.65
11	1.75	8	48	35	65	70.0855	73.92
12	1	12	35	50	20	77.1681	73.73
13	1.75	3	48	35	35	33.1624	32.09
14	2.5	4	35	20	20	44.9231	48.22
15	1	12	35	20	50	76.7179	74.15
16	1	12	60	20	50	87.2308	88.27

17	1.75	8	73	35	35	88.1111	92.56
18	1	12	35	50	50	98.8889	98.83
19	1	4	35	50	20	78.2252	72.54
20	1	12	60	50	50	91.7226	92.81
21	2.5	4	35	50	50	79.4929	84.41
22	1.75	8	48	35	35	82.3077	81.32
23	1	4	60	50	50	79.7166	75.59
24	1	12	60	20	20	73.2821	69.25
25	2.5	12	60	50	50	82.1029	79.23
26	1	12	60	50	20	78.0761	70.19
27	2.5	12	35	50	20	79.0455	77.54
28	2.5	12	60	20	20	69.1282	69.65
29	2.5	12	60	20	50	89.5897	87.75
30	2.5	4	60	50	50	75.5406	63.81
31	1.75	8	48	35	35	82.3077	81.32
32	1	4	60	20	20	53.4872	48.04
33	2.5	12	35	20	50	95.154	90.10
34	1	4	35	50	50	75.9135	79.73
35	2.5	4	35	20	50	50.5641	50.89
36	2.5	4	60	20	20	54.2051	50.24
37	2.5	12	60	50	20	51.3796	57.54
38	1	4	35	20	50	38.1538	33.15
39	1.75	8	48	35	35	82.3077	81.32
40	1.75	8	48	35	35	82.3077	81.32
41	1	4	60	50	20	57.9418	70.89
42	2.5	4	35	50	20	78.0611	78.14
43	2.5	12	35	50	50	98.6577	101.71

44	1.75	8	23	35	35	99.8291	96.56
45	2.5	12	35	20	20	71.2821	69.52
46	1	4	35	20	20	25.8462	29.56
47	1.75	8	48	35	35	82.3077	81.32
48	3.25	8	48	35	35	67.4359	67.36
49	1.75	8	48	35	35	82.3077	81.32
50	2.5	4	60	20	50	40.9744	50.43

3.10 Statistical Analysis

Analysis of variance (ANOVA) as presented in table 5, further confirmed the model's strength. The quadratic model was statistically significant, with a high F-value (21.40) and a p-value less than 0.0001, indicating that the model terms reliably explain the variations in phenol removal (Abonyı, Anıagor, Menkıtı, & Sciences, 2020). Among the individual factors, pH (B), concentration (D), and time (E) showed the most significant effects ($p < 0.0001$). Dosage (A) and temperature (C), while not individually significant ($p > 0.05$), were involved in several significant interaction terms, notably AC, AD, and CD, highlighting their contextual importance. Several interaction terms such as BD, BE, and CD also exhibited strong significance, indicating that phenol adsorption is governed not only by individual parameters but also by their combined effects. The model showed a high R^2 value (0.9365), with an adjusted R^2 of 0.8928 and predicted R^2 of 0.7837, demonstrating strong predictive power and internal consistency (Kamranfar et al., 2023). The adequate precision of 18.571 further confirmed the reliability of the model (Wu et al., 2019), while a low coefficient of variation (8.39%) indicated high experimental precision (Abdi, 2010; Marques, 2020). Also the Coefficient of variation (CV) is the ratio of the standard deviation to the mean (Abdi, 2010). The higher the coefficient of variation the greater the level of dispersion around the mean (Arachchige, Prendergast, & Staudte, 2022). The lower the value of the coefficient of variation (CV), the more precise the estimate (Körbahti & Tanyolaç, 2008). It measures the reproducibility of the model. If the value of the CV is less than 10% then the model can be considered reasonably reproducible. (Chowdhury et al., 2012). The coefficients of variation (CV) values obtained from the data analysis as presented in table 5 is 8.39 thus suggesting a good precision and high reliability of the experiment performed.

Diagnostic plots in figure 11 and 12, further validated the model's adequacy. The normal residual plot showed that residuals were approximately normally distributed, supporting the validity of ANOVA assumptions (Kozak, Piepho, & science, 2018). The predicted vs. actual plot demonstrated strong linearity, with most data points clustering closely along the diagonal, confirming that the model predictions aligned well with observed values (Gaffney, 2004).

Table 5. ANOVA for response surface quadratic model (RH)

Source	**Sum of Squares**	**df**	**Mean Square**	**F Value**	**p-value Prob > F**	
Model	15383.76	20	769.19	21.40	< 0.0001	Significant
A-dosage	*64.50*	*1*	*64.50*	*1.79*	*0.1908*	
B-pH	*3233.36*	*1*	*3233.36*	*89.96*	*< 0.0001*	
C-Temp	*40.05*	*1*	*40.05*	*1.11*	*0.2998*	

D-conc.	*2968.58*	*1*	*2968.58*	*82.60*	*< 0.0001*
E-Time	*1598.49*	*1*	*1598.49*	*44.47*	*< 0.0001*
AB	*6.42*	*1*	*6.42*	*0.18*	*0.6756*
AC	*541.95*	*1*	*541.95*	*15.08*	*0.0005*
AD	*341.12*	*1*	*341.12*	*9.49*	*0.0045*
AE	*1.71*	*1*	*1.71*	*0.047*	*0.8290*
BC	*7.11*	*1*	*7.11*	*0.20*	*0.6598*
BD	*959.16*	*1*	*959.16*	*26.69*	*< 0.0001*
BE	*641.52*	*1*	*641.52*	*17.85*	*0.0002*
CD	*811.20*	*1*	*811.20*	*22.57*	*< 0.0001*
CE	*12.32*	*1*	*12.32*	*0.34*	*0.5628*
DE	*25.89*	*1*	*25.89*	*0.72*	*0.4030*
A^2	*538.37*	*1*	*538.37*	*14.98*	*0.0006*
B^2	*1108.89*	*1*	*1108.89*	*30.85*	*< 0.0001*
C^2	*347.10*	*1*	*347.10*	*9.66*	*0.0042*
D^2	*14.60*	*1*	*14.60*	*0.41*	*0.5289*
E^2	*794.81*	*1*	*794.81*	*22.11*	*< 0.0001*
Residual	1042.30	29	35.94		
Lack of Fit	*1042.30*	*2*	*47.38*		
Pure Error	*0.000*	*7*	*0.000*		
Cor Total	16426.06	49			

Std. Dev.	6.00	R-Squared	0.9365
Mean	71.46	Adj R-Squared	0.8928
C.V. %	8.39	Pred R-Squared	0.7837
PRESS	3553.10	Adeq Precision	18.571

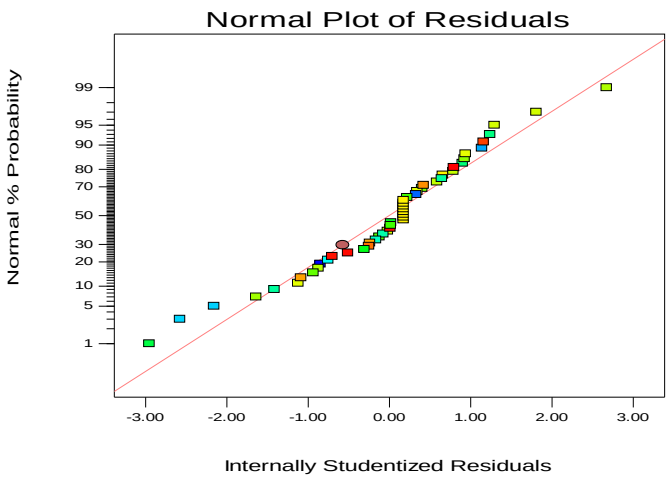

Figure 11. Normal Residual plot for uptake of phenol by RH

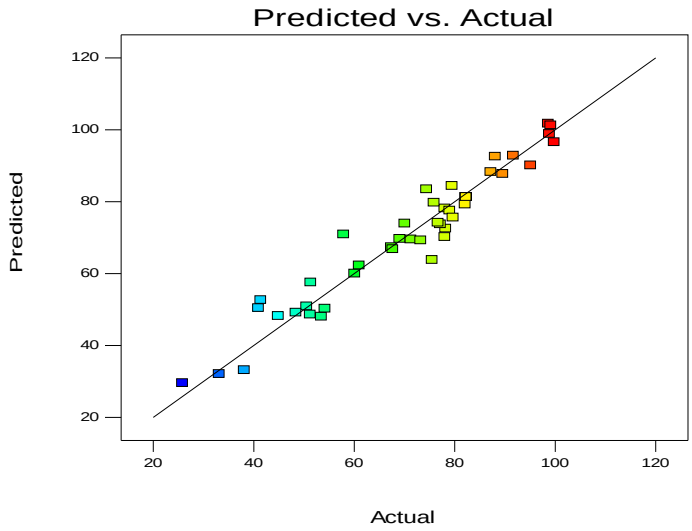

Figure 12. Predicted vs. Actual plots for phenol uptake by RH

3.11. CCD Regression Model for Phenol Adsorption

Multiple regression analysis was used to correlate the response (phenol percentage removal) with the five variables studied using a second order polynomial equation. The quadratic regression models for phenol uptake by RH is represented by equations 14 – 15. The regression model derived from the CCD data initially included all main, interaction, and quadratic terms. The full model equation revealed positive contributions from pH, concentration, and time, while certain interactions such as AC, AD, and BD negatively impacted the response. After removing statistically insignificant terms, a refined regression model was established as stated in equation 15, retaining only significant linear and interaction effects. This simplified model still accurately described the system, with pH (B), concentration (D), and time (E) retaining their dominant positive influence. The presence of significant quadratic terms for A^2, B^2, C^2, and E^2 indicates curvature in the response surface, suggesting that these parameters have optimal values beyond which adsorption efficiency begins to decline (Alsharief et al., 2024).

The response surface quadratic model equations are:

$$Y_{RH}(\%) = +81.32 + 1.27 * A + 9.63 * B - 1.00 * C + 8.61 * D + 6.32 * E - 0.45 * AB - 4.12 * AC - 3.26 * AD - 0.23 * AE - 0.47 * BC - 5.47 * BD + 4.48 * BE - 5.03 * CD - 0.62 * CE + 0.90 * DE - 4.12 * A^2 - 7.49 * B^2 + 3.31 * C^2 + 0.68 * D^2 - 5.01 * E^2 \quad (14)$$

For the model terms, P-Value less than 0.05 (Tables 5) implies that the model term is significant (Basu, Monal, & Pinaki, 2012). On removing the insignificant model terms, the quadratic models for the phenol uptake become.

$$Y_{RH}(\%) = +81.32 + 9.63 * B + 8.61 * D + 6.32 * E - 4.12 * AC - 3.26 * AD - 0.23 * AE - 5.47 * BD + 4.48 * BE - 5.03 * CD - 0.62 * CE - 4.12 * A^2 - 7.49 * B^2 + 3.31 * C^2 - 5.01 * E^2 \quad (15)$$

3.12. The Three Dimensional (3-D) Response Surface plot

To better understand the interaction effects, a series of three-dimensional (3D) response surface plots were generated. These plots visually confirmed and extended the statistical findings (Abonyı et al., 2020). From figure 13, the plot of dosage and concentration showed increased phenol uptake with rising concentration and moderate to high dosage levels, consistent with the positive coefficients of D and the interactive influence of A. In the dosage - temperature plot from figure 14, a moderate temperature enhanced removal at higher dosage levels, illustrating the significance of the AC interaction. The dosage - pH plot from figure 15 highlighted a steep rise in efficiency with increasing pH, particularly at moderate dosages. This aligns with the highly significant effect of pH and the observed interaction with dosage.

The concentration - pH surface from figure 16, demonstrated a strong synergistic effect, where slightly alkaline pH combined with high phenol concentrations yielded optimal removal. Similar trends were observed in the concentration - temperature plot from figure 17, though temperature played a less prominent role. The

temperature - pH surface from figure 18 illustrated how both variables influenced removal efficiency interactively, with certain combinations producing favorable outcomes. Contact time, a critical factor, consistently enhanced adsorption when combined with either concentration, dosage, or pH, as shown in the corresponding plots from figure 19 - 21 respectively. Notably, the time - pH plot revealed that prolonged contact time under alkaline conditions maximized phenol removal, aligning with both the regression model and the ANOVA. Collectively, these results confirm that phenol adsorption onto rice husk is a multifactorial process governed by both main and interaction effects. The combination of statistical modeling, diagnostic validation, and surface response visualization offers a comprehensive understanding of the system dynamics, providing a solid foundation for optimization and scale-up in wastewater treatment applications as confirmed by (Abonyı et al., 2020).

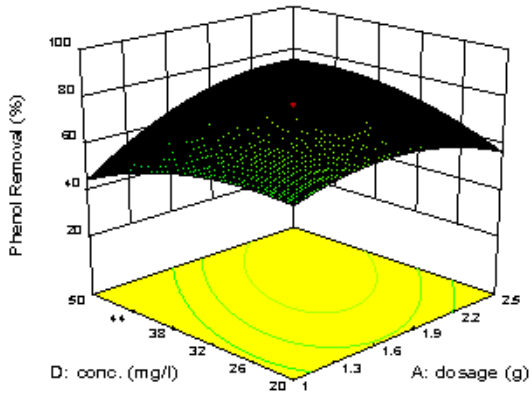

Figure 13. 3D plot of the effect of effluent concentration and adsorbent dosage

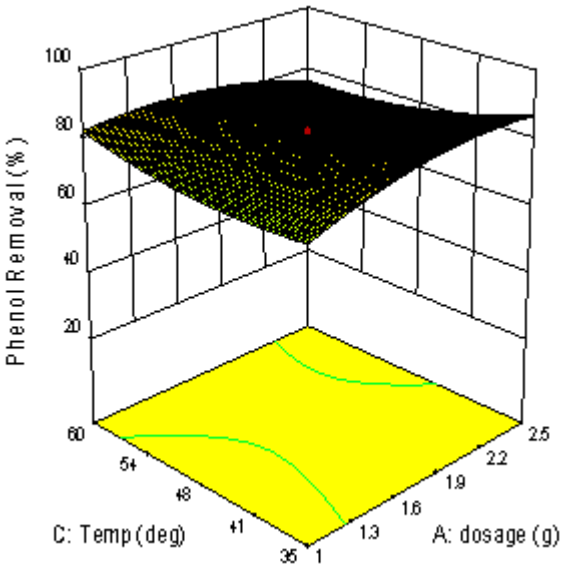

Figure 14. 3D plot of the effect of Effluent temperature and adsorbent dosage

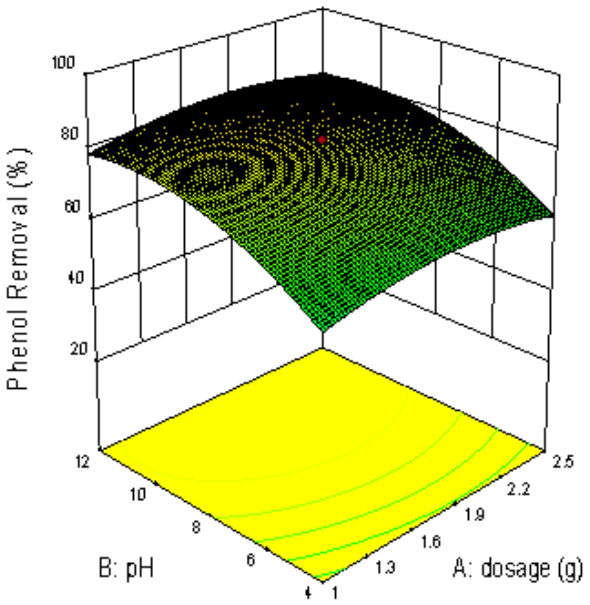

Figure 15. 3D plot of the effect of pH and adsorbent dosage

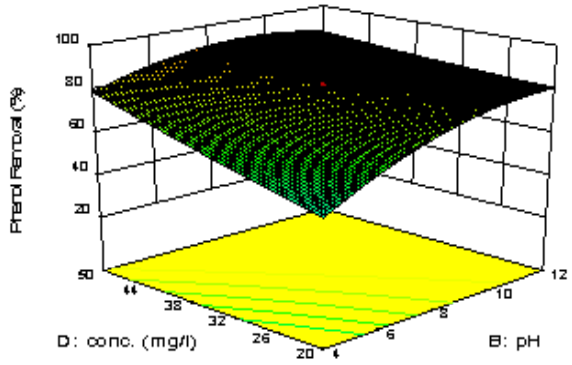

Figure 16. 3D plot of the effect of Effluent concentration and Effluent pH

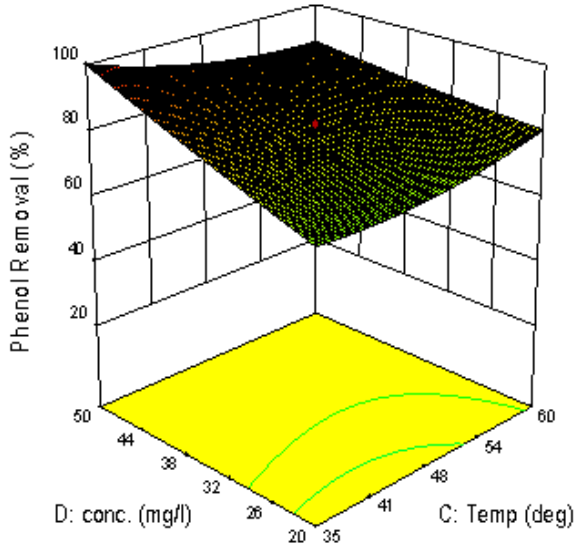

Figure 17. 3D plot of the effect of Effluent concentration and Effluent temperature

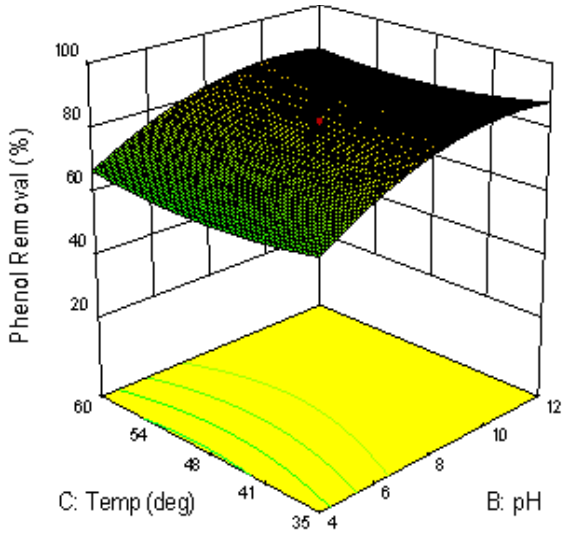

Figure 18. 3D plot of the effect of Effluent temperature and Effluent pH

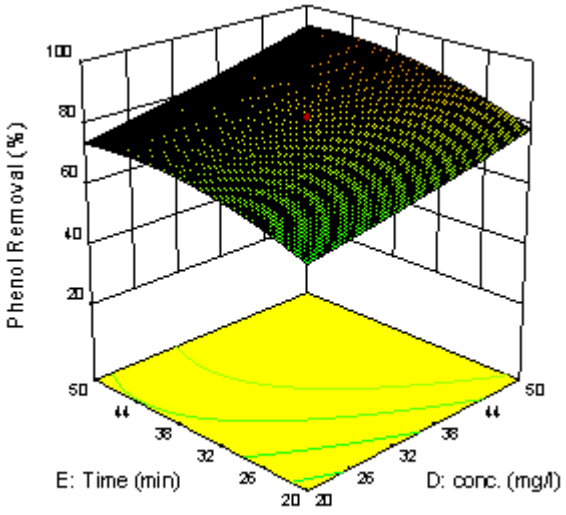

Figure 19. 3D plot of the effect of contact time and Effluent concentration

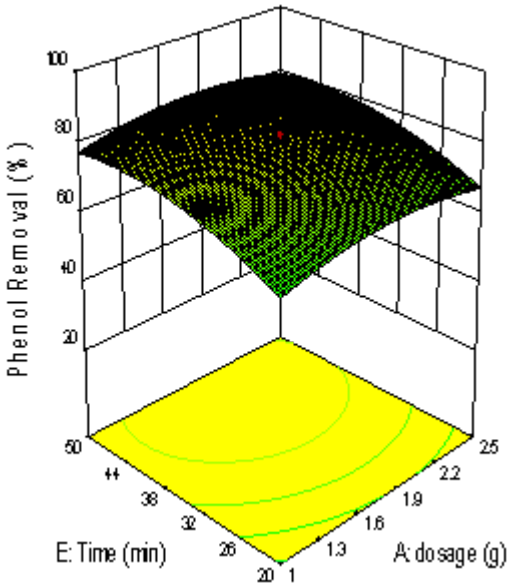

Figure 20. 3D plot of the effect of contact time and adsorbent Dosage

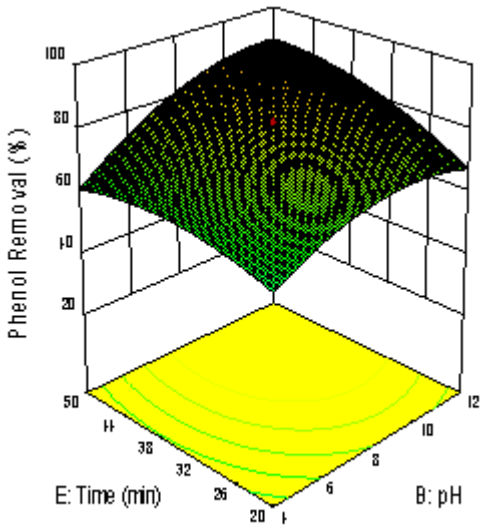

Figure 21. 3D plot of the effect of contact time and Effluent pH

3.13 Comparison with Literature

The adsorption capacity obtained in this study (66.5 mg/g) is comparable to or higher than many agro-waste-based adsorbents reported for phenol removal, which typically range between 20-60 mg/g (Bhatnagar & Sillanpää, 2010; Hameed & Rahman, 2008). The high removal efficiency (99.83%) and relatively short equilibrium time (~35 min) further demonstrate the effectiveness of carbonized rice husk. The superior performance observed can be attributed to the combined thermal and chemical activation, which enhances pore development, surface area, and the availability of active adsorption sites (Mishra et al., 2023). In addition, the application of response surface methodology (RSM) enables efficient optimization of process variables and accounts for interaction effects, providing improved performance compared to conventional single-factor approaches (Reji & Kumar, 2022). In all, the results highlight the potential of carbonized rice husk as a competitive and sustainable adsorbent for phenol removal from wastewater systems.

Conclusions

This study demonstrated the effective removal of phenol from pharmaceutical wastewater using carbonized rice husk (RH) as a low-cost and sustainable adsorbent. Batch adsorption experiments revealed that process parameters such as pH, initial phenol concentration, and contact time significantly influenced adsorption performance, with optimum removal achieved at pH 5 and equilibrium attained within 35 minutes.

Equilibrium analysis showed that the Langmuir isotherm best described the adsorption process, with a maximum adsorption capacity of 66.5 mg/g, indicating monolayer adsorption on a relatively homogeneous surface. Kinetic studies confirmed that the pseudo-second-order model provided the best fit, suggesting that surface interactions govern the adsorption process. Thermodynamic analysis further established that the adsorption is spontaneous and exothermic, with the mechanism predominantly driven by physical interactions.

The application of Response Surface Methodology (RSM) using Central Composite Design (CCD) enabled effective modeling and optimization of the process, achieving a maximum phenol removal efficiency of 99.83%. The high coefficient of determination (R^2 = 0.9365) and statistical significance of the model confirm its reliability in predicting system behavior.

In all, the findings highlight the potential of carbonized rice husk as an efficient, eco-friendly adsorbent for phenol removal from complex wastewater systems. The integration of low-cost materials with advanced optimization techniques provides a promising approach for sustainable wastewater treatment and offers potential for practical application and industrial application.

Funding

This research did not receive any specific grant from funding agencies in the public, commercial, or not-for-profit sectors.

Conflicts of Interest

The authors declare no conflict of interest.

Nomenclature:

q_e – adsorption capacity

q_t – adsorption capacity at time t

C_0 – initial concentration

Ce – equilibrium concentration

RH – Rice husk

References

Abdi, H. J. E. o. r. d. (2010). Coefficient of variation. *1*(5), 169-171.

Abonyı, M. N., Anıagor, C. O., Menkıtı, M. C. J. S. J. o. E., & Sciences, N. (2020). Statistical modelling of the adsorptive dephenolation of petroleum industry wastewater using ionic liquid treated clay. *38*(3), 1099-1112.

Alsharief, H. H., Alatawi, N. M., Al-Bonayan, A. M., Alrefaee, S. H., Saad, F. A., El-Desouky, M., & El-Bindary, A. J. E. T. (2024). Adsorption of Azorubine E122 dye via Na-mordenite with tryptophan composite: batch adsorption, Box–Behnken design optimisation and antibacterial activity. *45*(17), 3496-3515.

Arachchige, C. N., Prendergast, L. A., & Staudte, R. G. J. J. o. A. S. (2022). Robust analogs to the coefficient of variation. *49*(2), 268-290.

Ayawei, N., Ebelegi, A. N., & Wankasi, D. J. J. o. c. (2017). Modelling and interpretation of adsorption isotherms. *2017*(1), 3039817.

Basu, J., Monal, D., & Pinaki, G. J. A. o. A. S. R. (2012). Statistical optimization for the prediction of ibuprofen adsorption capacity by using microwave assisted activated carbon. *4*(2), 1053-1060.

Beker, U., Ganbold, B., Dertli, H., Gülbayir, D. D. J. E. C., & Management. (2010). Adsorption of phenol by activated carbon: Influence of activation methods and solution pH. *51*(2), 235-240.

Bhatnagar, A., & Sillanpää, M. J. C. e. j. (2010). Utilization of agro-industrial and municipal waste materials as potential adsorbents for water treatment—a review. *157*(2-3), 277-296.

Chen, H., Zhao, J., Wu, J., & Dai, G. J. J. o. h. m. (2011). Isotherm, thermodynamic, kinetics and adsorption mechanism studies of methyl orange by surfactant modified silkworm exuviae. *192*(1), 246-254.

Chowdhury, Z., Zain, S. M., Khan, R. A., Ahmad, A., Khalid, K. J. R. J. o. A. S., Engineering, & Technology. (2012). Application of response surface methodology (RSM) for optimizing production condition for removal of Pb (II) and Cu (II) onto kenaf fiber based activated carbon. *4*(5), 458-465.

Chulliyil, H. M., Hamdani, I. R., Ahmad, A., Al Shoaibi, A., Chandrasekar, S. J. R. i. S., & Interfaces. (2024). Enhanced moisture adsorption of activated carbon through surface modification. *14*, 100170.

Coates, J. J. E. o. a. c. (2000). Interpretation of infrared spectra, a practical approach. *12*, 10815-10837.

da Silva Aires, F. I., Dari, D. N., Freitas, I. S., da Silva, J. L., de Matos Filho, J. R., dos Santos, K. M., . . . da Silva Sousa, P. J. D. W. (2024). Advanced and prospects in phenol wastewater treatment technologies: unveiling opportunities and trends. *4*(1), 20.

Dąbrowski, A., Podkościelny, P., Hubicki, Z., & Barczak, M. J. C. (2005). Adsorption of phenolic compounds by activated carbon—a critical review. *58*(8), 1049-1070.

Elmorsi, T. M. J. J. o. E. P. (2011). Equilibrium isotherms and kinetic studies of removal of methylene blue dye by adsorption onto miswak leaves as a natural adsorbent. *2*(6), 817-827.

Foo, K. Y., & Hameed, B. H. J. C. e. j. (2010). Insights into the modeling of adsorption isotherm systems. *156*(1), 2-10.

Gaffney, S. J. (2004). *Probabilistic curve-aligned clustering and prediction with regression mixture models*: University of California, Irvine.

Hall, K. R., Eagleton, L. C., Acrivos, A., Vermeulen, T. J. I., & fundamentals, e. c. (1966). Pore-and solid-diffusion kinetics in fixed-bed adsorption under constant-pattern conditions. *5*(2), 212-223.

Hameed, B., & Rahman, A. J. J. o. h. m. (2008). Removal of phenol from aqueous solutions by adsorption onto activated carbon prepared from biomass material. *160*(2-3), 576-581.

Hammam, A., Zaki, M. S., Yousef, R. A., & Fawzi, O. J. A. i. e. b. (2015). Toxicity, Mutagenicity and carcinogenicity of phenols and phenolic compounds on human and living organisms [A Review]. *9*(8), 38-49.

Ho, Y.-S., & McKay, G. J. P. b. (1999). Pseudo-second order model for sorption processes. *34*(5), 451-465.

Ho, Y.-S. J. J. o. h. m. (2006). Review of second-order models for adsorption systems. *136*(3), 681-689.

Húmpola, P., Odetti, H. S., Fertitta, A. E., & Vicente, J. L. J. J. o. t. C. C. S. (2013). Thermodynamic analysis of adsorption models of phenol in liquid phase on different activated carbons. *58*(1), 1541-1544.

Kamranfar, S., Damirchi, F., Pourvaziri, M., Abdunabi Xalikovich, P., Mahmoudkelayeh, S., Moezzi, R., & Vadiee, A. J. S. (2023). A partial least squares structural equation modelling analysis of the primary barriers to sustainable construction in Iran. *15*(18), 13762.

Khan, A. H., Aziz, H., Khan, N., Hasan, M. A., Ahmed, S., Farooqi, I., . . . Technology. (2022). Impact, disease outbreak and the eco-hazards associated with pharmaceutical residues: a critical review. *19*(1), 677-688.

Körbahti, B. K., & Tanyolaç, A. J. J. o. h. M. (2008). Electrochemical treatment of simulated textile wastewater with industrial components and Levafix Blue CA reactive dye: Optimization through response surface methodology. *151*(2-3), 422-431.

Kozak, M., Piepho, H. P. J. J. o. a., & science, c. (2018). What's normal anyway? Residual plots are more telling than significance tests when checking ANOVA assumptions. *204*(1), 86-98.

Lagergren, S. (1898). About the theory of so-called adsorption of soluble substances.

Langmuir, I. J. J. o. t. A. C. s. (1918). The adsorption of gases on plane surfaces of glass, mica and platinum. *40*(9), 1361-1403.

Lin, K., Pan, J., Chen, Y., Cheng, R., & Xu, X. J. J. o. H. M. (2009). Study the adsorption of phenol from aqueous solution on hydroxyapatite nanopowders. *161*(1), 231-240.

Marques, V. J. R. B. d. B. (2020). Coefficient of variation: a new approach for the study in maize experiments.

Mishra, S., Dhada, I., Haldar, P. J. A. w. t. v.-a. p. t., economic, & aspects, s. (2023). Rice Husk: from agro-industrial to modern applications. 295-320.

Reji, M., & Kumar, R. J. I. J. M. R. (2022). Response surface methodology (RSM): An overview to analyze multivariate data. *9*(4), 241-248.

Rengaraj, S., Moon, S.-H., Sivabalan, R., Arabindoo, B., & Murugesan, V. J. W. m. (2002). Agricultural solid waste for the removal of organics: adsorption of phenol from water and wastewater by palm seed coat activated carbon. *22*(5), 543-548.

Stuart, B. H. (2004). *Infrared spectroscopy: fundamentals and applications*: John Wiley & Sons.

Temkin, M. J. A. p. U. (1940). Kinetics of ammonia synthesis on promoted iron catalysts. *12*, 327-356.

Villegas, L. G. C., Mashhadi, N., Chen, M., Mukherjee, D., Taylor, K. E., & Biswas, N. J. C. P. R. (2016). A short review of techniques for phenol removal from wastewater. *2*(3), 157-167.

Wang, L., Shi, C., Pan, L., Zhang, X., & Zou, J.-J. J. N. (2020). Rational design, synthesis, adsorption principles and applications of metal oxide adsorbents: a review. *12*(8), 4790-4815.

Wu, H., Li, J., Jia, Y., Xiao, Z., Li, P., Xie, Y., . . . Zhao, M. J. J. o. A. M. i. C. (2019). Essential oil extracted from Cymbopogon citronella leaves by supercritical carbon dioxide: antioxidant and antimicrobial activities. *2019*(1), 8192439.

Yuh-Shan, H. J. S. (2004). Citation review of Lagergren kinetic rate equation on adsorption reactions. *59*(1), 171-177.

1.
2.